

---

## EXPERIMENTAL ANALYSIS OF SINGLE AND THREE-STAGE HEAT PIPE WITH THREE FLUIDS FOR COOLING OF ELECTRONIC DEVICES

M.VELLIANGIRI<sup>1</sup>, G. SURESHKANNAN<sup>2</sup>, M. KARTHIKEYAN<sup>3</sup>

<sup>1,2,3</sup> *Department of Mechanical Engineering, Coimbatore Institute of Technology- Coimbatore Tamilnadu- INDIA*

### Abstract

*An electronic device and energy storage device such as a super and ultra-capacitor are kept cool by a single or three-stage cascade heat pipe: selected heat pipe materials, primary and secondary fluids. Cascade heat pipes designed, built, and tested single and three fluid cascade heat pipes with heat inputs ranging from 100 to 200 W. The axial temperature difference is studied, and the evaporator and condenser temperatures are measured using a thermocouple and connected to an Agilent Data Logger. In multistage heat pipe experiments, each stage reached a steady state after 35 seconds. Heat pipe temperature, thermal resistance, and heat transfer were predicted. The primary fluid (water) merit number  $4.26 \times 10^9$  is 25 times higher than ethanol merit number  $166.3 \times 10^6$  and acetone merit number, but ethanol had a higher latent heat of evaporation than water. The operating range (100 to 220 deg C) was suitable for energy storage devices.*

Key words: *Experimental Analysis, Three fluid Heat Pipe, cascade system, design of heat pipe*

### Introduction

[1] The heat pipe is widely utilized in various energy storage devices and computer processors, such as microprocessors, electronics devices, electrical drives and solar energy storage devices. The heat pipe is also used in supercapacitors and ultra-capacitors, among other things. The design and analysis of multistage heat pipes are required to use advanced applications such as capacitor cooling and evacuated glass tube heat pipe. Increasing or reducing the temperature of any electrical equipment is dependent on the amount of heat generated as a result of energy storage and consumption [2]. As a result, an appropriate cooling mechanism is essential for regulating the system temperature and ensuring that the performance requirements are met [3]. Additionally, variable heat load heat pipes are necessary because the heat load varies depending on whether the energy is consumed or stored. On the other hand, previous heat pipes were not suited for variations in heat load in relation to the specified design value [4]. Because of this, the goal of this research is to build an appropriate cascade heat pipe for variable heat load input to energy and energy storage systems [5]. Following are the four stages that must be completed to pick appropriate materials for heat pipes, fluid properties, and geometry parameters that meet the design requirements. 1) Selection of heat pipe materials, such as the container; 2) selection of tube materials; 3) selection of working fluid wick materials; 4) selection of appropriate materials and volumes for the condenser and evaporator; and 5) prediction of performance limits. [6] [7]. This means that it is important to go through the process of designing the Cascade heat pipe system. It is necessary to make numerous decisions, many of which are intertwined with the design and performance procedures, which must be completed. It is possible that the

choice of working fluids in the case of heat will be limited by pipe compatibility, or that the materials employed would need to be specified beforehand [8]. If the performance constraints are not met despite careful selection of all parameters and materials, it may be essential to turn to other alternatives to meet the performance requirements. In addition, two more variables are taken into consideration while designing heat pipes: the amount of fluid charge and the time it takes for the heat pipe to begin operating. Another critical decision, the number of fluid charges at each stage, is difficult to make or must be done through experimentation. The condenser capacity will be reduced due to overcharging, whilst the artery may be dried out due to undercharging. Providing an extra fluid reservoir that will absorb surplus fluid while also being non-required by the primary wick structure [11],[12] is the research topic at hand.

### Design Methodology and Experimental Setup

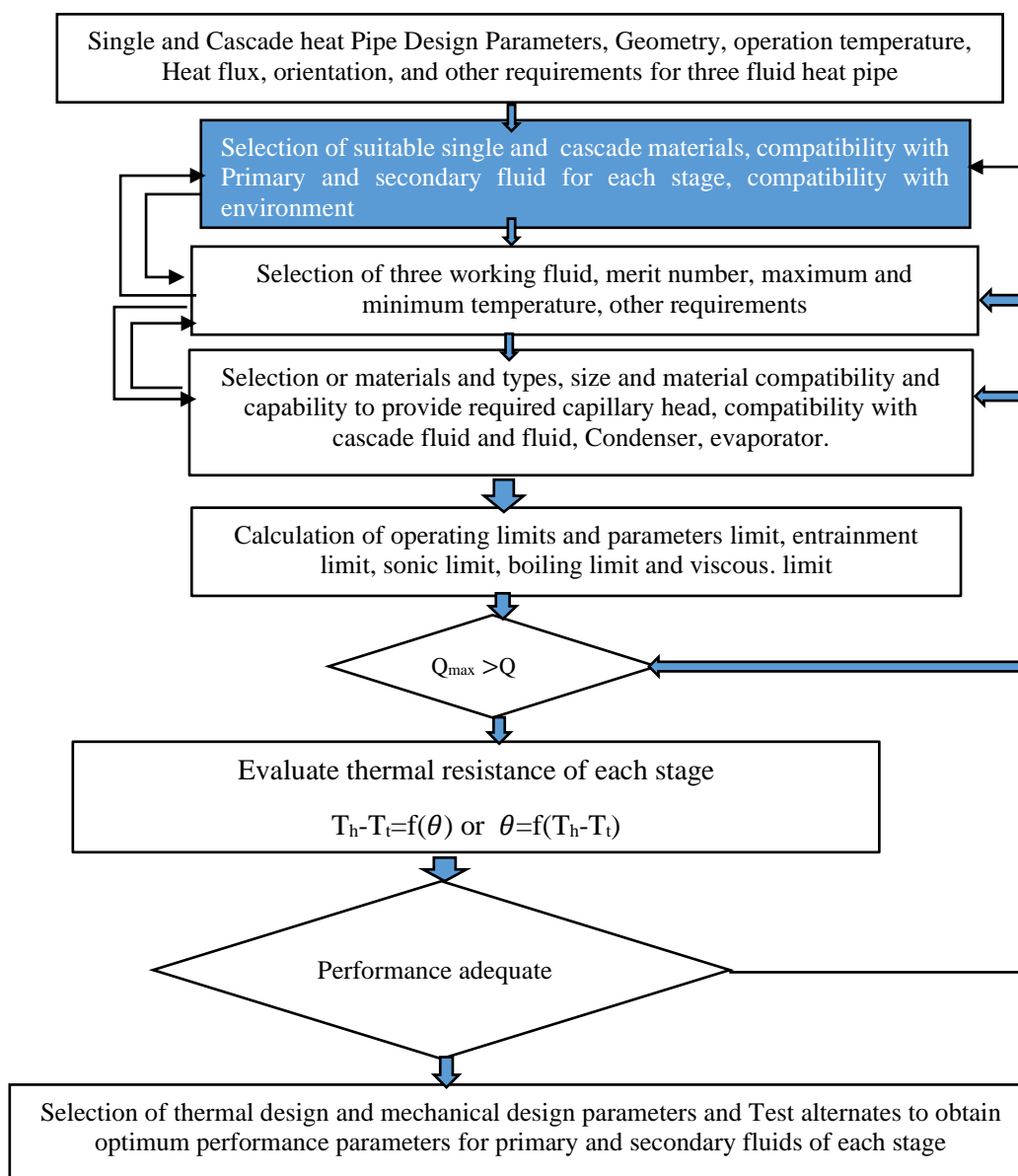


Figure 2.1 Design Procedure methodology for cascade heat pipe

With arterial wicks, it is vital to ensure that, if the working fluid of the vessel is exhausted, it will be immediately replenished; this is known as priming [6] in the medical community. As a result, the design methodology for single and cascade heat pipes was developed in accordance with the literature and the requirements of single and multistage heat pipe design [13]. As illustrated in figure 2.1, the cascade heat pipe design concept is ineffective when selecting appropriate devices and procedures. Systematically, the design approach was followed, and the properties of the required materials and fluids are shown in the following tables: 1 and 2. The current study has involved numerous rigorous investigations that have resulted in the development and commercialization of heat pipes for various applications in record time. Step two consists of picking a working fluid set and forecasting the most appropriate operating temperature. In terms of the fluid selected, the operational materials and wick and the type of wick are chosen. The optimal working fluid compatible with these materials is determined [14]. [15]. Choosing a wick capable of supplying the desired capability head capacity is necessary. This cycle is performed as many times as necessary until the criteria have been met. In the following step, the temperature difference between the condenser and the evaporator is projected at the maximum permitted value [16]. Once these conditions have been met, the comprehensive design process can begin in earnest. The heat pipe and the condenser and evaporator are specified when the unit is required to work against the "g" force [15]. Specifications will include weight restrictions and temperature differences between the evaporator and condenser. Table 2 contains a list of suitable working fluids that have been selected.

### Design Procedure

The design of single and cascade heat pipes is based on some essential steps are involved they are:

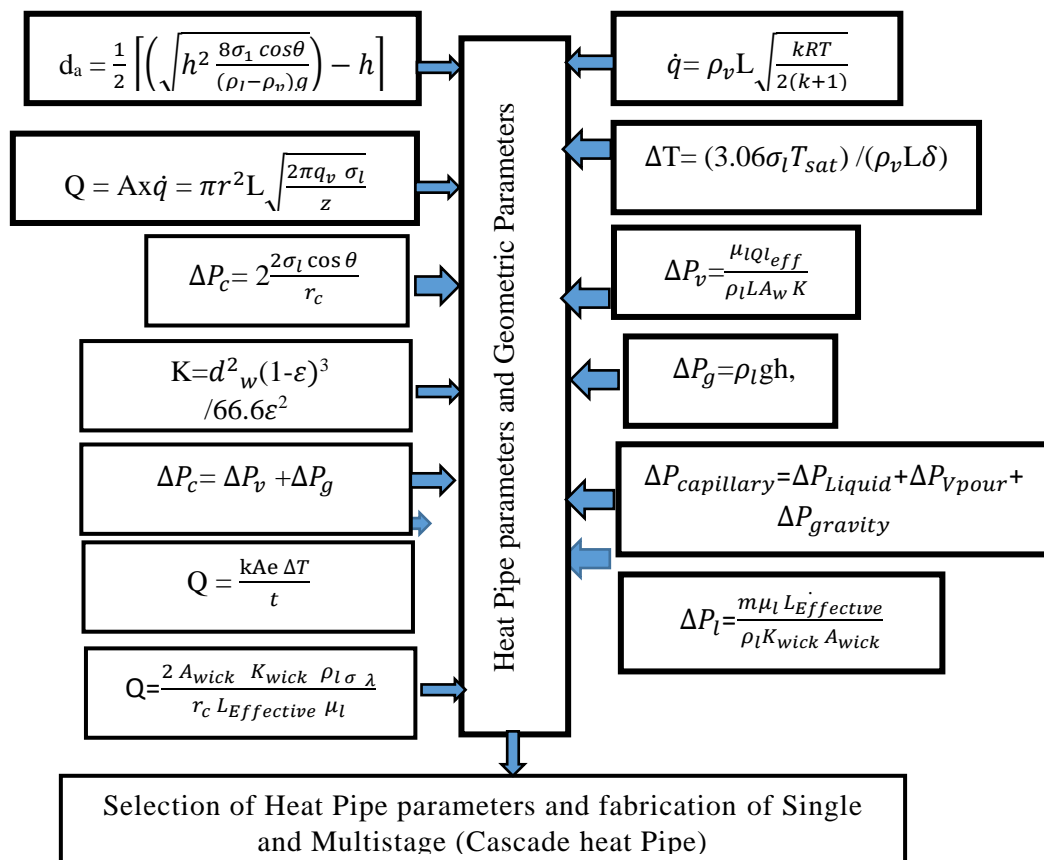


Figure 2.2 single and cascade Heat Pipe Design Procedure

The greatest circumference of the heat source, the pipe 'd<sub>a</sub>' is determined using the process outlined below, and all parameters are predicted systematically. Specifically, where d<sub>a</sub> represents

the maximum diameter of the artery, his represents the vertical height from its base, - represents the fluid's contact angle, l represents the surface tension of the fluid, and  $\rho_l$  and  $\rho_v$  represent the densities of liquid and vapour, respectively. As illustrated in Figure 2.1, the Heat Pipe design procedure can be easily understood. The following parameters and details of the heat pipe's specification, including geometry, operating temperature, heat load, orientation, and other details such as where it is to be used in space, are determined. Figure 2.1: Heat Pipe Design Procedure, the temperature range of the working fluid, is defined. The sonic limit for the liquids is obtained by applying the equation for maximum heat flux to the specified temperature range of the working fluid ( $Q_{max}$ ). R represents the gas constant, and k denotes the specific heat ratio of the system. The fluid can be selected if the heat flux exceeds the needed heat flux. The maximal heat flow ( $Q_{max}$ ) is determined without entrainment [17].

$$Q_{max} = A\dot{q} = \pi r^2 L \sqrt{\frac{2\pi q_v \sigma_l}{z}} \tag{1}$$

Where: Z is one of the characteristic dimensions of the liquid and vapour interface about 0.16, it is required to predict the Q and equal to compare with  $Q_{max}$  or higher than the heat load of the pipe to be designed the fluids pass this limit[6]. In addition to that working limit is checked by using the Merit Number shown in Table 1. To avoid nucleation in the wick, the superheat may be obtained, and  $\Delta T$  is calculated shown Figure 2.2 Where  $\delta$  is a thermal layer, having a value of  $15\mu m$ . The fluid having the highest value for  $\Delta T$  is the most suitable one for the application. Priming Factor for the fluid is determined from plots of Temperature verses, priming factor.

It is preferable to use the fluid with a more excellent value of priming factor if it meets all of the other parameters. The thickness and weight of the container are determined by the weight and vapour pressure of the fluid. The parameters listed above and any other specifications needed are used to decide which working fluid to use. The type of wick is chosen depending on a number of characteristics, and the homogenous wick and arterial wick are developed. The design process is used to compute the capillary pressure in the capillary.  $\Delta P_c$ . Where  $r_c$  is the radius of the wick and is the contact angle for wetting fluids, which is equal to zero, the pipe will function if the pressure equals the pressure drop caused by the vapour flow and gravitational pressure combined. Predict the amount of vapour. The equation illustrated in Figure 2.2 is used to compute the amount of force required for vapour flow. As a result of utilizing the equation,  $P_v$  is the wick area and K is estimated,  $l_{eff}$  is the length of pipe-1/2(Length of evaporator+ size of condenser), and  $l_{eff}$  is computed (2).

$$K = d_w^2 (1-\varepsilon)^3 / 66.6\varepsilon^2 \tag{2}$$

$d_w$  is the wick diameter,  $\varepsilon$  is the volume fraction of the solid phase in the wick. The value is substituted in equation (2), the pressure required for the movement against gravity,  $\Delta P_g = \rho_l gh$ , where h is the height of motion against gravity. The  $P_c$  is calculated by using the equation (3)

$$\Delta P_c = \Delta P_v + \Delta P_g \tag{3}$$

The wick area is comprised of a number of wicks.  $A_w$  is computed since all of the other variables in the equation are known except for  $A_w$ . In the event when  $A_w$  is more than the pipe diameter. The heat flow across it is calculated using the equation for heat flow over the wick to determine the wick's thickness. The equation predicts the heat transfer coefficient (Q) to the evaporator. The consistency is measured in millimetres (m). Q represents the heat load, while  $A_e$  represents the evaporator area. The temperature drop that is permitted is denoted by the symbol T. When you combine the conductivities of the solid material in the wick with the conductivities of the working fluid in the wick, you get k. Pressure drop is determined using the basic equation  $P_c = \text{sum of various pressure drops}$  to find the maximum pressure drop value. These equations are also used to

determine the number of arteries in a body. A large amount of information on the properties of the liquid and the wick is required for the heat pipe design. The information is not readily available, and it is necessary to seek through literature and handbooks to find it. A heat pipe's maximum heat pipe power is ranked according to its Merit number [6] when the heat pipe's capillary limitation is present. (According to the equation, the capillary limit was reached when the sum of the liquid, vapour, and gravitational pressure drops equalled the capillary pumping capability, which was projected by utilizing the equation. The merit number does not account for the pressure drops caused by vapour and gravity. It is assumed that the capillary pumping capability equals the liquid pressure drop. The fluid pressure drop across a heat pipe was computed using the equation provided. Figure 2 illustrates this. 2. In this equation,  $P_l$  is the liquid pressure drop, which is assumed to be equal to the wick pumping capability,  $L_{\text{effective}}$  is the effective length,  $K_{\text{wick}}$  is the wick permeability,  $A_{\text{wick}}$  is the wick area, the mass flow rate is equal to the heat transfer rate and the wick pumping capability is defined as  $P_l = (2\sigma) / r_c$ , where  $r_c$  is the pore diameter. The most significant heat transfer when only the liquid pressure drop is considered can be calculated by combining the three equations above and solving for  $Q$  with the help of this equation. A list of materials based on the design procedure and calculation method and the selection of the material required based on various tests comments is presented in table1. The materials list based on the operating low and maximum temperature is shown in table1.

**Table 1** Operating Temperature, operating max temperature working fluid and Envelope Materials for Heat Pipe

Operating Min Temp., °C	Operating Max Temp., °C	Working Fluid	Envelope Materials	Comments
20	280, short term to 300	Water	Copper, Monel, Nickel, Titanium	Aluminium, steels, stainless steels and nickel are not compatible
100	350	Naphthalene	Al, Steel, Stainless Steel, Titanium, Cu-Ni	380°C for the short term. Freezes at 80°C
200	300, short term to 350	Therminol	Al, Steel, Stainless Steel, Titanium	. Incompatible with Copper and Cu-Ni
200	400	AlBr <sub>3</sub>	Hastelloy	Aluminium is not compatible. Freezes at 100°C

The design and materials selection is made by using design methodology. Some conflicts mainly depend on the material deterioration of one component and other component parameter selection procedures. Compatibility with wick and container materials, good thermal stability, wettability of wick and wall surface, suitable vapour pressure not too high or too low, Large latent heat, Good thermal conductivity, High surface tension, Low viscosity of liquid as well as vapour and acceptable freezing and pour points are predicted and list of working fluid as shown in Table 2

Table 2 List of working Fluids boiling point, Use fuel range and Merit number for heat pipes

Sl. No	Description of fluids	Boiling points, °C	Useful range, °C	Merit number W/m <sup>2</sup>
3	Ammonia	-33	-60 to 100	449.8x10 <sup>6</sup>
4	Pentane	28	-20 to 120	134.7x10 <sup>6</sup>
5	Acetone	57	0 to 120	364.6x10 <sup>6</sup>
6	Ethanol	78	0 to 120	166.3x10 <sup>6</sup>
7	Heptane	98	0 to 150	123.8x10 <sup>6</sup>
8	Methanol	64	10 to 130	377.9x10 <sup>6</sup>
9	Flutec PP2	76	10 to 160	17.7x10 <sup>6</sup>
10	Water	100	30 to 200	4.26x10 <sup>9</sup>

Source: <https://www.1-act.com/merit-number-and-fluid-selection>.

Heat pipe requires considering a single property; fluids are evaluated by a combination of properties influencing the working of heat pipes called Merit number, it is defined as

$$N_l = \frac{\sigma_l \rho_l}{\mu_l} \text{ W/m}^2 \tag{4}$$

Where  $\sigma, \rho, \mu$  and  $L$  are the surface tension, density, viscosity and Latent heat of the fluid. The dimension of the merit number is W/m<sup>2</sup>. Effectively merit number indicates the heat transport capacity of the fluid[18]. The sectional area required for transporting a given thermal load is directly proportional to the merit number. The merit number(MN) as a function of temperature is shown in Figure: 2 for several typical heat pipe working fluids[18][13]. The figure shows that it is obvious why it is chosen as the heat pipe working fluid whenever possible[15]. Water merit number is approximately ten times higher than everything else except the liquid metal is, and it means that it will carry ten times more power than other working fluids

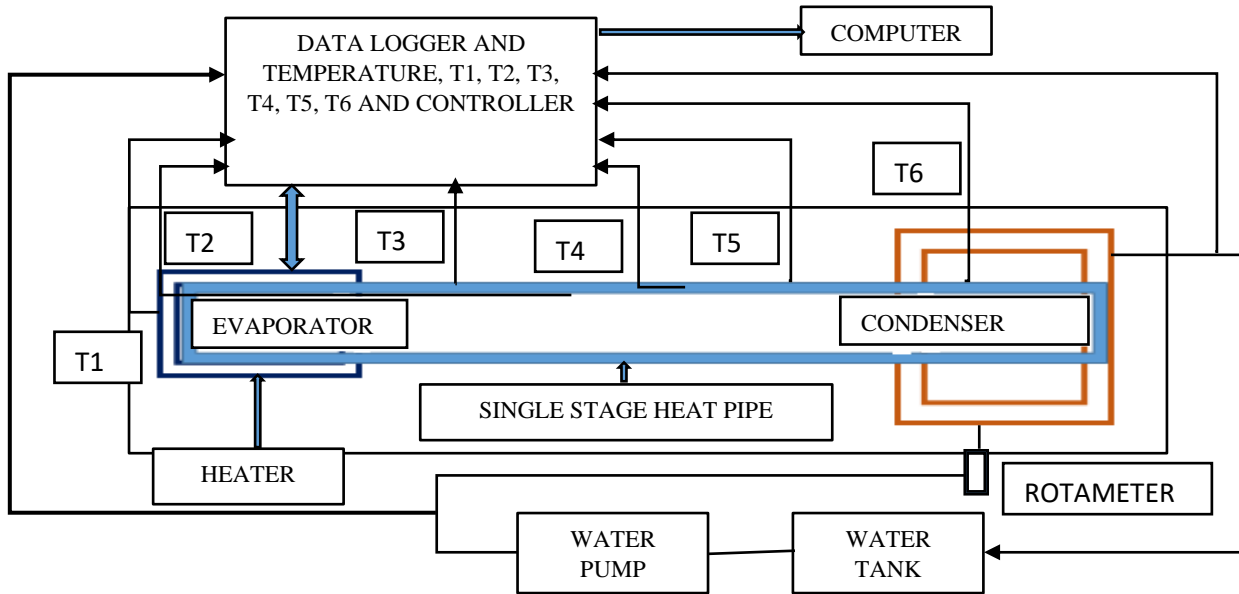
The experimental layout of single and multistage heat pipes are shown in Figures 2.3.and 2.4. They are 1) The working fluid 2) The wick and capillary structure and container. As cascade thermosiphon heat pipes are required to work at various temperatures from 4k to 2300k, different fluids are required for other temperature bands. For example, helium was used in the low-temperature range of 4k. Liquid oxygen, Nitrogen are used in the next band. Water, Ammonia and alcohol were used in the field of 300 to 500K. Unique materials are required in the range of 600 to 600k. Above this temperature, sodium, lithium and similar materials are used. More than two dozen fluids are in use as working fluid. Similarly, the arrangement and material for wick also vary as per the applications; more than a dozen materials are used to be compatible with the various fluids. The above difficulty always arises in selecting a suitable combination of material and liquid.

### Experimental Layout

Figure 2.3 and Figure 2.4 depict a schematic diagram of the single and multistage heat pipe experiment setups, respectively. The experimental design consists of the evaporator, adiabatic section, and other heat pipe components such as single and multistage heat pipes, as shown in the figure. The Datalogger depicted in Figures 2.3 and 2.4 are used to link temperature measuring devices such as K type thermocouples, the cooling water circulation system mass flow rate, and the cooling water temperature. Figure 2.4 depicts the components of a cascade heat pipe and a thermocouple, and a heat source. The heat input from the first stage heat pipe condenser to the second and second-stage condensers is represented by the third stage heat input in Figure 2.4. The components in the experimental setup with a primary heat pipe stage 1 and a second stage heat pipe are placed into the first stage, as illustrated in Figure 2.4, as those in the setting where

there is a secondary heat pipe stage 1. For the experimental purpose, an autotransformer controlled a single and multistage heater. A steady watt is delivered to the system with a regulator, in which amps substitute a regulator contains the electrical component and volt input. In the primary reservoir, this heater is located at the bottom of the tank.

Figure 2.3 Experimental layout of Single-stage heat pipe



T1-Heater Temperature, T2-Evaporator Temperature, T3-Condenser temperature, T4, T5, T7 – water outlet temperature, T8-Water inlet temperature.

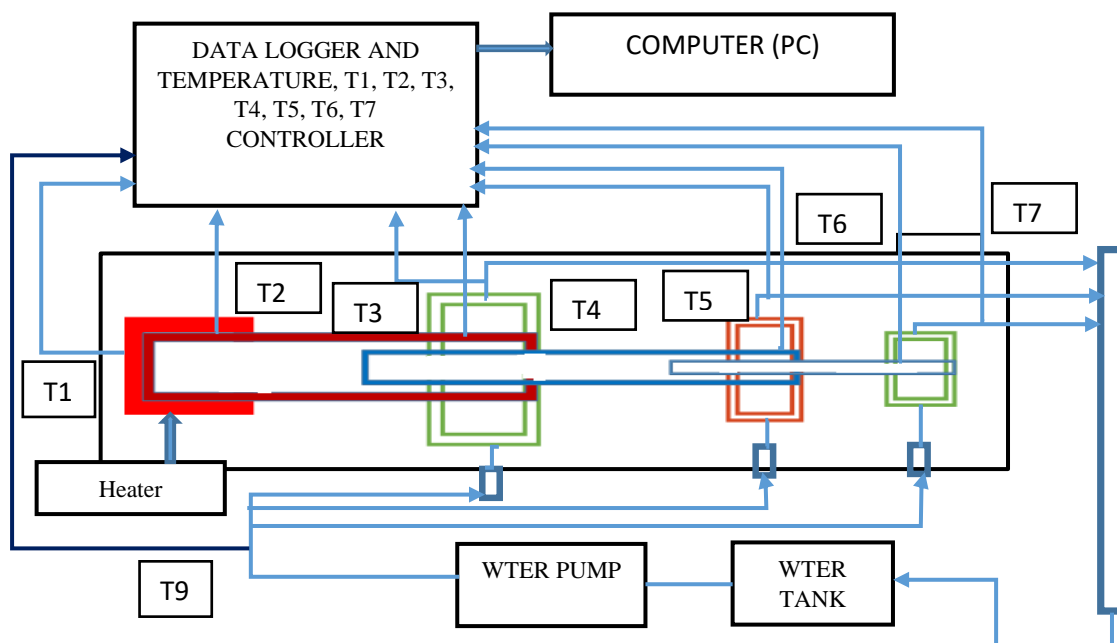


Figure 2.4 Experimental layout of the multistage stage heat pipe

T1-Heater Temperature, T2-Evaporator Temperature, T3-Condenser temperature, T4, T5, T7, T8– water outlet temperature, T9-Water inlet temperature.

Table: 3 Specification of Single and Multistage Heat Pipes

SL.No	Description	Values (mm)	Area mm <sup>2</sup>	Exp1-Fluid1
1	Cascade Heat Pipe Length	1000	28260	Water
SL.No	Description	Stage 1	Stage 2	Stage 3
1	Length of Heat Pipe	400	400	400
2	Evaporator length	100	100	100
3	Adiabatic section	200	200	200
4	Condenser	100	100	100
5	OD of heat Pipe	30	20	14
6	ID of the Heat Pipe	26	16	10
7	Wick Type Screen Mesh( 4 layer)	50/cm	50/cm	50/cm
8	<b>Merit Number ( W/m<sup>2</sup>)</b>	<b>166x10<sup>6</sup></b>	<b>166x10<sup>6</sup></b>	<b>166x10<sup>6</sup></b>
9	<b>Boiling Point deg C</b>	<b>78</b>	<b>78</b>	<b>78</b>
9	Mesh wire diameter	0.08 mm	0.08 mm	0.08 mm

### Experimental Methodology

The schematic diagram of the experiments and setup is shown in Figures 2.3 and 2.4. The components in the experimental design are an evaporator and condenser.

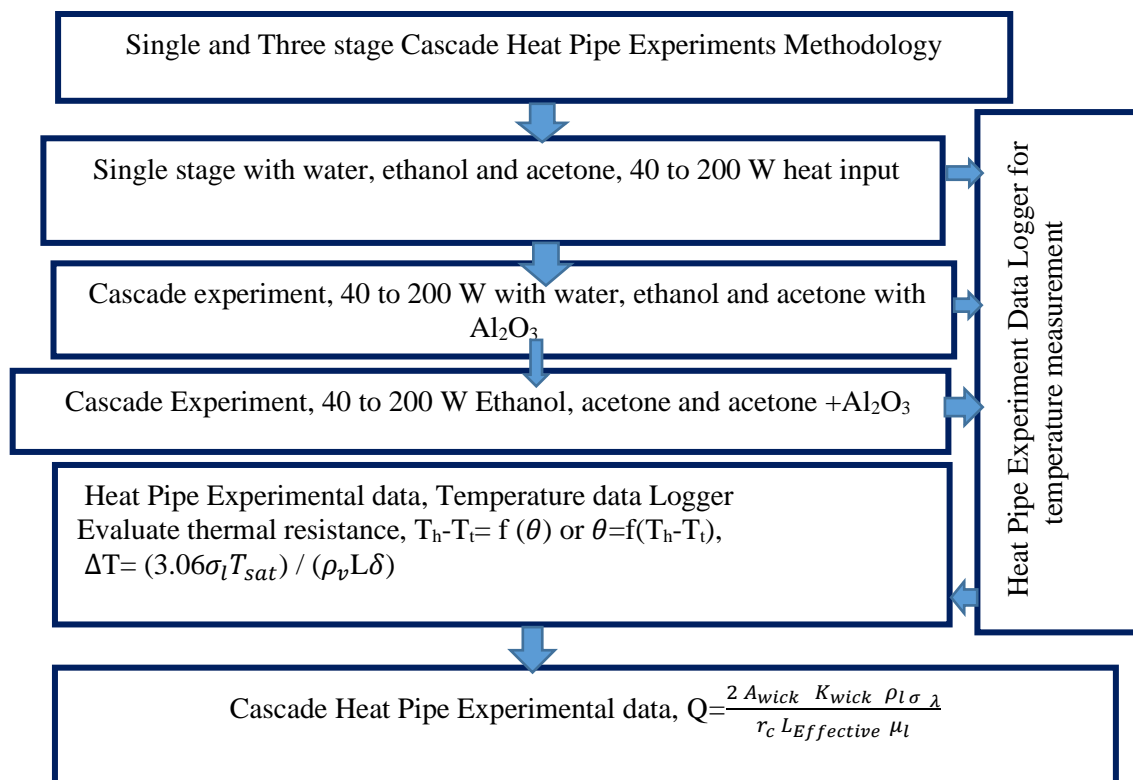


Figure 2.5 Experimental Layout of the cascade heat pipe



The experimental technique used the following experiments with a single-stage with water, ethanol, and acetone under various heat loads ranging from 40 to 200 W. Thermal resistance, the efficiency of the heat pipe, and temperature variation with axial distance are all discussed about the experimental data. The same method was continued with a cascading heat pipe filled with a mixture of water, ethanol, and acetone. The heater, which is connected to a temperature controller, is located at the evaporator portion. The first reservoir contains distilled water as a working fluid. In contrast, the secondary pool contains secondary working fluid containing ethanol, with the third fluid being acetone as the final working fluid. The heater, which has a power of 1000W, is attached to the bottom of the primary reservoir, which has a surface area of 65mm\*80 mm, and the maximum amount of heat flux that can be delivered to the system is 192.308\*10<sup>3</sup> w/m<sup>2</sup>. Heat pipe experiments were carried out to investigate the axial temperature. They were divided into two phases: the first phase consisted of three experiments for a single-stage heat pipe with variable heat load conditions. The second phase consisted of a multistage heat pipe with variable heat load conditions. A copper tube with a diameter of 30 mm and a length of 1000 mm was used to construct a single-stage heat pipe, with the ends of the tube being sealed with end caps on both ends. A filling tube was used to charge the working fluids, which served as one of the end caps. The wick part was constructed from a 4-layer 50/cm mesh copper screen that was fastened to the inner tube and held in place by a guided arrangement to maintain its fixed position. The heat pipe was evacuated using a vacuum pump. A 10<sup>-4</sup> bar pressure was maintained at 120 degrees Celsius for approximately 4 hours to remove the non-condensable accumulated in the tube. Once the heat pipe had been chilled with ice, a capillary tube was used to inject the necessary amount of working fluid (210 ml) into the system, controlled by manipulating a vacuum valve (7.38 kPa).

Following that, the capillary tube was pinched and sealed. In accordance with their relative positions in the system, the evaporator, adiabatic, and condenser sections each have a length of 100, 600, and 300 millimetres (mm). Heat transfer capacity of the heat pipe was increased by bracing 40 (70x70) flat fins of 0.6 mm thickness, which were mounted on the condenser section and maintained the adiabatic section of the heat pipe under isothermal boundary conditions, which were achieved through the use of glass wool insulation.. The same technique was continued, and the produced cascade (Multistage) heat pipe and three-stage heat pipe were fabricated, tested, and displayed in Figure 2.3 as examples of what was accomplished. Table 1 contains the technical specifications for both single-stage and multistage heat pipes. A resistance heater with a 1500W power output, a wattmeter, and an auto-transfer are all included in the experimental setup (Fig. 2.3), which is also responsible for providing the necessary power supply to the heaters. The thermocouple readings at various places along the heat pipe were recorded using a system based on national instruments (NI). The temperature response at multiple positions along the axial distance was measured using thermocouples of the K-type (10 numbers in total). Figure 3 depicts the physical arrangement of thermocouples.

### **Experimental Procedure**

The following tests were done using the experimental methodology. We used one stage of 100, 600 and 300-mm-long evaporators and condensers with water, ethanol and acetone to get testing results. The heat pipe adiabatic portion was kept isothermal by utilizing glass wool insulation and 40 (70x70) flat fins of 0.6 mm thickness braced on the condenser section. The exact process was used to manufacture the cascade (multistage) heat pipe depicted in Figure 2.2. Table 1 shows the single and multistage heat pipe specifications. An auto transfer is used to power the heaters, as shown in Figure 2.2. The thermocouple measurements were recorded using a

National Instruments (NI) system. The temperature response was measured using K-type thermocouples (10 numbers). Fig. 3 shows the thermocouple setup.

The bay a two-T type thermocouple with a data logger was used to measure the cooling water's inlet and output temperatures. A control valve measured the steady-state mass flow rating of cooling water. An autotransformer controlled the power supply to the heater and adiabatic sections. The variable transformer changes the heat input from 60 to 300 W. The data acquisition system monitored the cooling water and heat pipe temperatures. The mass flow rate of water was measured in a steady-state heat pipe. The same method was used with three different fluids, with similar results. The cascade heat pipe experiment used water, ethanol, and acetone as stage 1, 2, and 3 fluids.

### Results and Discussions

The experimental and analytical calculations reveal the following performance parameters depicted in the following figures. Axial temperature difference, thermal resistance, and overall heat transfer coefficient of the heat pipe's performance can all be explained in temperature differences. Using the equation  $R=T/Q$ , we were able to calculate the thermal resistance of the heat pipe. In this equation,  $t$  represents the temperature differential between the evaporator and condenser walls, and  $q$  represents the volume of the heat pipe in cubic metres. Several expressions for estimating thermal resistance for different portions of the heat pipe are presented in Table 3. The heat pipe is separated into three portions for ease of installation. Figure 4.1 depicts the variation in thermal resistance of the heat pipe filled with copper nano-particles suspension and the copper nano-particles suspension.

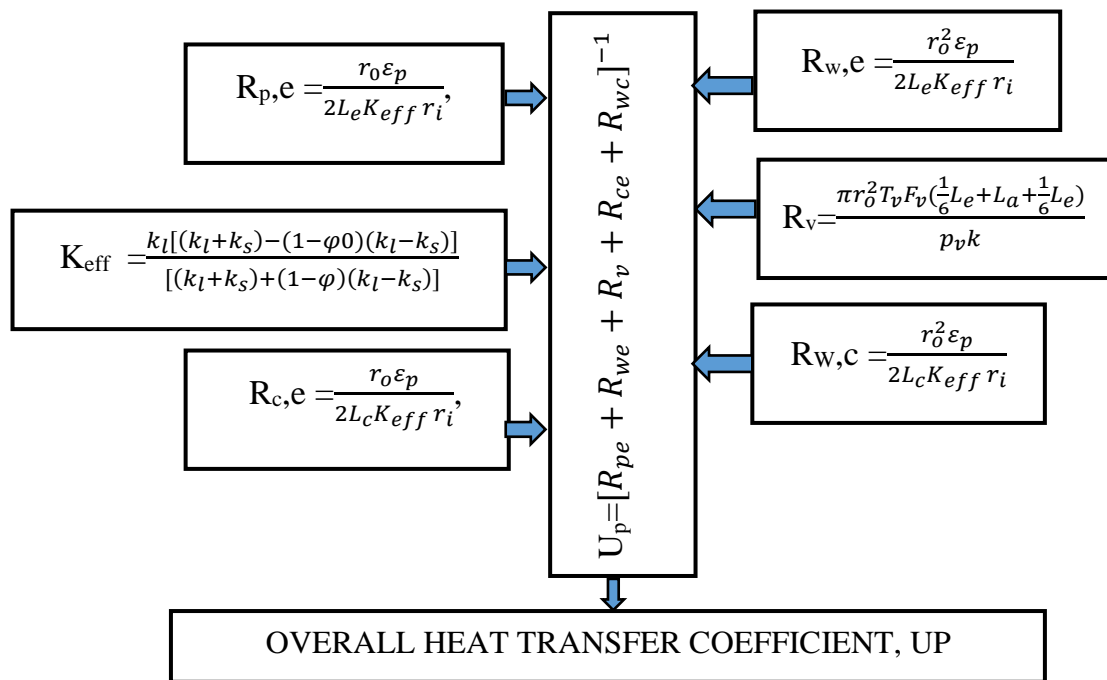


Figure 4.1. Overall heat Transfer Coefficient calculation procedure for single and multistage (cascade system) heat Pipe.

The heat resistance of single and multistage stages was anticipated and discussed in the figure based on the procedure described above. The thermal resistance trend demonstrates that a heat pipe's thermal resistance reduces as heat input increases. The experimental results showed

that employing a different fluid in the heat pipe resulted in lower thermal resistance for higher heat input. Due to the activation of several nucleation sites in the evaporator section, the thermal resistance has been reduced, allowing the nucleate boiling regime to be extended to highly high heat fluxes and the performance of the multistage to be improved.

**Error Estimates of Single And Multistage Heat Pipe Experiment**

It is vital to analyze the error estimates for both the experimental part and the impact of the data and analysis on the final result. The temperature measurements, namely coolant flow rate and the wattmeter were the leading causes of experimental uncertainty. This error analysis was completed and summarised for the accuracy of flow measurement, which is approximately 2.5 percent, and the accuracy of the thermocouple, which is roughly 5 percent at zero degrees Celsius. The maximum uncertainty of the wattmeter is around 1.5, and the method described by the author follows the error analysis method provided by Holman. Additional to delays of the heat flux and the heat transfer coefficient, which were anticipated and tabulated as shown in Table 3, and uncertainties calculated by Eqs. 1, 2 which are shown in Table 4, there were uncertainties computed by Eqs. 1, 2 which are shown in Table 5.

$$q_c = \sqrt{\left(\frac{\partial q}{\partial Q} w_q\right)^2 + \left(\frac{\partial q}{\partial D} w_D\right)^2 + \left(\frac{\partial q}{\partial L_c} w_{L_c}\right)^2} \tag{1}$$

$$h_c = \sqrt{\left(\frac{\partial h_c}{\partial q_c} w_{q_c}\right)^2 + \left(\frac{\partial h_c}{\partial \Delta T} w_{\Delta T}\right)^2} \tag{2}$$

Which shows that uncertainties are within a reasonable limit of 5-6%.

The symbols  $w_q, w_D, w_{L_c}, w_{q_c}, w_{\Delta T}$  are the uncertainties in the heat flow rate, diameter, condenser-length condenser-heat flux and temperature drops, respectively.

Table 4 Uncertainty of Heat Flux and Heat transfer coefficient of single-stage and cascade heat pipe.

	Heat pipe with water		Heat pipe with ethanol and acetone Cascade heat pipe	
Heat input	Uncertainty of Heat Flux single stage (%)	Uncertainty of heat transfer coefficient single stage (%)	Uncertainty of Heat Flux cascade system (%)	Uncertainty of heat transfer coefficient cascade system (%)
100	6.01	6.34	6.22	6.51
150	6.0	6.11	6.34	6.39
200	5.3	5.14	6.03	6.24
250	5.89	5.96	6.07	6.35
275	5.92	6.01	6.24	6.39

**Over All Heat Transfer Coefficient, Result, and Discussion**

The above procedure was used to calculate the overall heat transfer coefficient shown in Figure 2.4  $U_p = [R_{pe} + R_{we} + R_v + R_{ce} + R_{wc}]^{-1}$  (5)

Temperature Transfer in the Condenser Section To provide an additional evaluation of the heat transfer performance of the heat pipe, the heat transfer coefficient in the condenser

section was determined with base fluid for both single-stage and multistage heat pipe configurations using base fluid.  $Q_{out} = m C_p \Delta T$ ,  $q_c = Q_{out} / (d l c)$ , and  $q_c = Q_{out} / (d l c)$  may be used to compute the experimental heat transfer coefficient at the condenser section of single and multistage condensers, respectively. Where  $m$  denotes the mass of the water flow and  $C_p$  denotes the specific heat of the water, respectively.  $T$  denotes the temperature differential caused by the water flow. A similar technique was followed to identify a cascade system. The heat output of a single-stage was determined by applying the equation

$$Q_c = (Q_{out1} = m C_p \Delta T) \tag{4}$$

$$Cascade\ system - Q_{cascade} = (Q_{out1} = m C_p \Delta T) + (Q_{out2} = m C_p \Delta T) + (Q_{out3} = m C_p \Delta T) \tag{5}$$

Where  $Q_{out1}$  is the heat transfer at stage 1,  $Q_{out2}$  is the heat transfer at stage 2,  $Q_{out3}$  is the heat transfer stage 3. Total Heat Transfer is  $Q_{out} = (Q_{out1} + Q_{out2} + Q_{out3})$ . The figure depicts the increase in the condensing heat transfer coefficient caused by adding two stages (multistage) with two different fluids, such as ethanol and acetone, to the system. Compared to a single-stage heat pipe, the results showed that the heat transfer coefficient of the multistage heat pipe altered with the number of stages. It is considered that the nature of the surface generated by the multistage as the convection area was extended was the most critical factor in the heat transfer enhancement in the evaporator and condenser sections. During the condenser section, the heat transfer coefficient is determined by the thickness of the liquid layer and the hydrodynamic parameters of the working fluid. It is possible to create a relationship between the Nusselt number, the Reynolds number, and the Prandtl number.

$$N_u = \frac{(h c_l)}{K} = 1.12 Re^{0.8} Pr^{0.7} \tag{8}$$

The correlation of Eq. 9 may be compared with the existing correlation for condensing water vapour in thermosiphon as a function of Reynolds number, see Figure

$$N_u = 5.03 Re^{1/3} Pr^{1/3} \tag{9}$$

Figure Shows the Nusselt number variation concerning the Reynolds number for the endless Prandtl number. The trend shows an enhancement in the Nusselt number with the increase in the Prandtl number and Reynolds number, which means that the rise in the Prandtl number leads to the enhancement of the Nusselt number. The figure shows a comparison of the experimental results of the heat pipe.

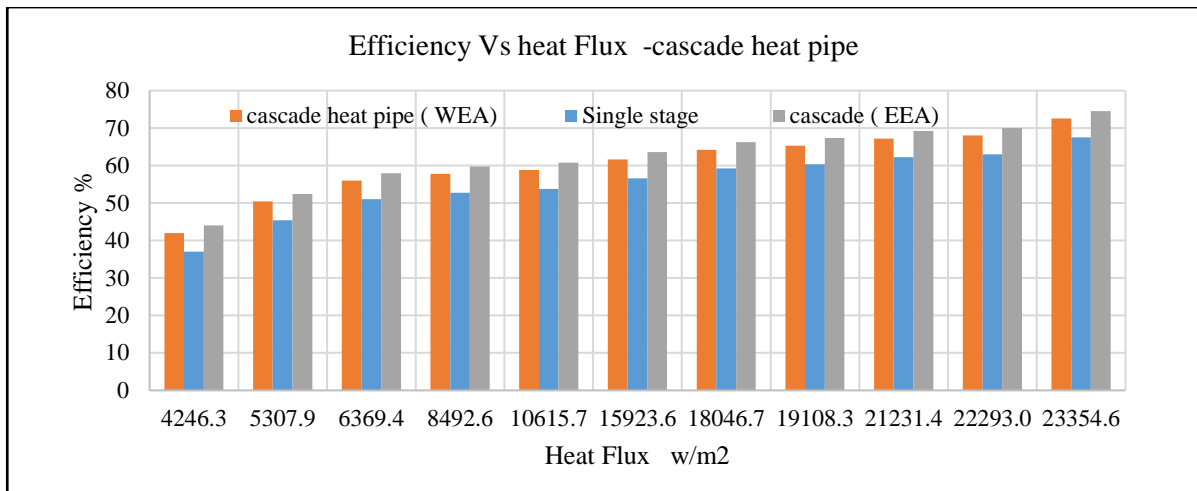


Figure 4.2 The variation of efficiency concerning Heat Input of cascade Heat Pipe

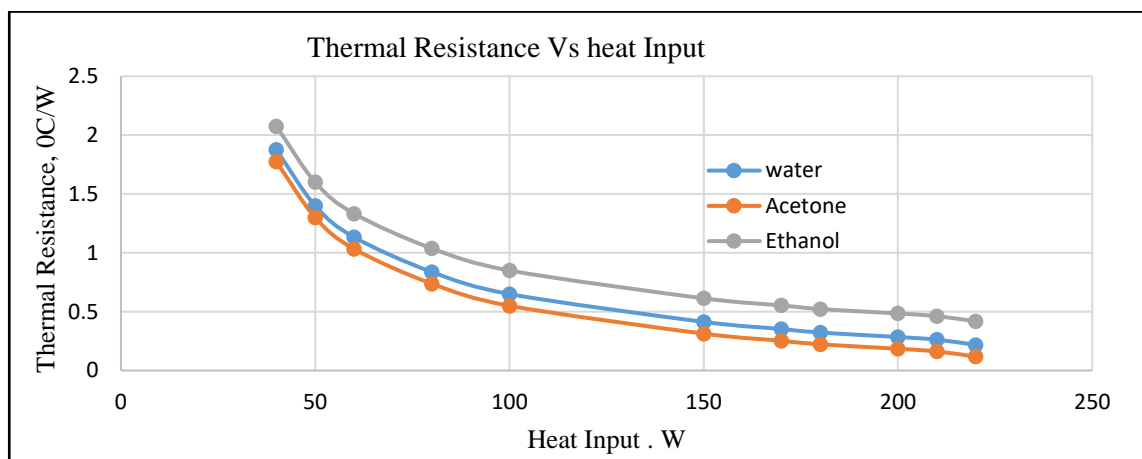
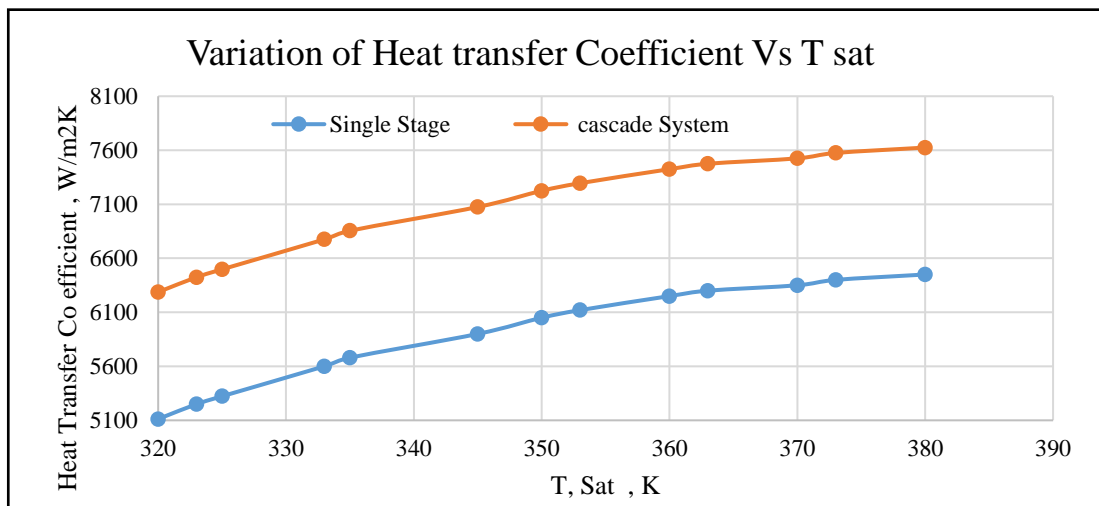


Figure 4.3 the variation of Thermal Resistance concerning Heat Input

Figure 4.2 depicts the variance in efficiency as a function of the heat flux. It can be shown that increasing the heat input results in increased inefficiency. Compared to Ethanol, Ethanol, and Acetone (EEA) fluid combination cascade heat pipe, the efficiency of Water, Ethanol, and Acetone (WEA) fluid combination cascade heat pipe is somewhat lower by 2.3 percent. When comparing the single-stage heat Pipe to the cascade heat Pipe, the single-stage heat Pipe was 5.2



percent less expensive. Thermal resistance decreases as the amount of heat applied increases, as illustrated in Figure 4.3. Figure 4.3 depicts the fluctuation in resistance as a function of the amount of heat applied. When the heat input to the water fluid heat pipe is increased, the thermal resistance of the water fluid heat pipe decreases.

Figure 4.3 comparison and study of variation of Heat Transfer coefficient vs T sat K  
As shown in figure 4.3, the variation in heat transfer coefficient with temperature (T sat (K)) is a function of temperature. It is possible to demonstrate that the heat transfer coefficient increases as the temperature rises in the laboratory. Cascade heat pipe heat transfer coefficient is 18.3 to 19.5 percent higher than that of a single-stage heat pipe compared to the latter. It was necessary to conduct a series of experiments in order to evaluate the heat transmission properties of the evaporator and condenser sections of the heat pipe, and the results were analysed. The amount of heat transmitted in the condenser portion is determined by the Reynolds number and the Prandtl number, which are both positive numbers. The interior fluid velocity and condensate liquid, as well as the hydrodynamic properties of the condensate liquid, are all critical in the condensing heat transmission of heat pipes, whether they are single or cascaded.

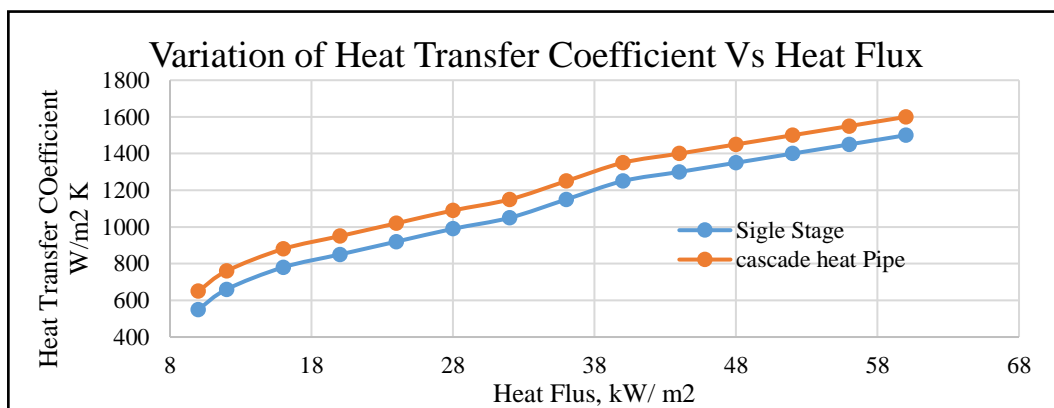


Figure 4.4 Comparison and study of Variation of Heat Transfer Coefficient Vs Heat Flux

Figure 4.4 depicts the relationship between heat transfer and coefficient of performance and heat flow. A series of single and multistage heat pipe experiments were carried out to investigate the heat transfer properties of the evaporator and condenser sections of the heat pipe, as seen in Figure 4.4. When the heat flux increases from 8.2 to 68.9 kW/m<sup>2</sup>, the heat transfer coefficient increases. Increases in heat flux or saturation temperature maximum of 23.10 percent cause a gradual increase in the overall heat transfer coefficient of the system, with the heat transfer coefficient increasing by 16.4 percent compared to a single-stage system due to a decrease in thermal resistance of the heat pipe.

## Conclusion

Experiments were conducted to understand better the heat transfer properties of both the evaporator and condenser sections of single and cascade heat pipes. Because of the relationship between Reynolds number and Prandtl number, heat transfer in the condenser portion of a single-stage with water fluid and ethanol fluid heat pipe is dependent on both of these

numbers. Single-stage heat pipe heat transfer is 18.3 percent lower than cascade heat pipe heat transmission because two low boiling point fluids are employed in the second and third stages, resulting in 18.3 percent lower heat transfer. The convection area of the cascade increased as the experimental examination progressed, and the heat transfer rate rose as well.

## Nomenclature

$G$	- Acceleration due to gravity,	$T_{water}$	- Water temperature, °C
$\infty$	- Ambient	$\nu$	- Kinematic viscosity, m <sup>2</sup> /s
$A_{vg}$	- Average		
$H$	- Heat Transfer Co Efficient	$N$	- Number of secondary tubes arranged
$B$	- Bottom wall	$Nu$	- Nusselt number, $hL/k$ , $hd/k$
$T_m$	- Bulk mean temperature	$Pr$	- Prandtl number, $\nu/\alpha$
$B$	- Co-efficient of volumetric expansion,	$pri$	- Primary coolant
$Q_{sides}$	- Convective heat loss	$Ra$	- Rayleigh number,
$Q_{top}$	- Convective heat loss	$sec$	- Secondary coolant
$T_{max}$	- Dimensionless temperature,	$A_h$	- Surface area of the heater, m <sup>2</sup>
$exp$	- Experimental	$A_1$	- Surface area of the primary tank, m <sup>2</sup>
$FN$	- Figure of Merit,	$A_2$	- Surface area of the secondary tubes,
$f$	- Fluid	$T_s$	- Surface temperature
$Gr$	- Grashoff number,	$\Delta T$	- Temperature difference surface, °C
$q_{pri}$	- Grashoff number,	$T$	- Temperature excess, $(T_h - T_\infty)$ , C
$q_{sec}$	- Heat,	$K_f$	- Thermal conductivity of the fluid, W/m-K
$q''$	- Heat flux (W/m <sup>2</sup> )	$\alpha$	- Thermal diffusivity of the fluid, m <sup>2</sup> /s
$Q_{in}$	- Heat input	$R_{th}$	- Thermal resistance, °C/W
$T_{heater}$	- Heater temperature, °C	$V$	- Voltage applied to the heater, Volts

## Acknowledgement

Dr A. S. Krishnan, Associate Professor, and Dr K. Marimuthu, Professor, Head of the Department of Mechanical Engineering, Coimbatore Institute of Technology, Coimbatore-641014, for his keen interest in timely motivation and inspiring guidance, as well as his constant encouragement with my work throughout all stages of the research, which enabled me to complete the examination successfully.

### Reference

- [1] I. A. Mhaisne, P. B. Borade, S. V Mohitwar, and A. A. Pawar, "Experimental Investigation Of Copper Sintered Heat Pipe Flow For Power Electronic Coolingby Vortex," pp. 50–54, 2015.
- [2] K. N. Shukla, A. B. Solomon, B. C. Pillai, B. J. R. Singh, and S. S. Kumar, "Thermal performance of heat pipe with suspended nano-particles," *Heat Mass Transf. und*

- Stoffuebertragung*, vol. 48, no. 11, pp. 1913–1920, 2012.
- [3] R. Hari and C. Muraleedharan, "Analysis of Effect of Heat Pipe Parameters in Minimizing the Entropy Generation Rate," *J. Thermodyn.*, vol. 2016, 2016.
- [4] S. Lips, V. Sartre, F. Lefevre, S. Khandekar, and J. Bonjour, "Overview of Heat Pipe Studies During the Period 2010-2015," *Interfacial Phenom. Heat Transf.*, vol. 4, no. 1, pp. 33–53, 2016.
- [5] R. Andrzejczyk, "Experimental investigation of the thermal performance of a wickless heat pipe operating with different fluids: Water, ethanol, and SES36. Analysis of influences of instability processes at working operation parameters," *Energies*, vol. 12, no. 1, 2019.
- [6] M. Narcy, S. Lips, and V. Sartre, "Experimental investigation of a confined flat two-phase thermosyphon for electronics cooling," *Exp. Therm. Fluid Sci.*, vol. 96, pp. 516–529, 2018.
- [7] P. K. Jain, "Influence of Different Parameters on Heat Pipe Performance, Sharmishtha Singh Hada under the guidance of Prof," *J. Eng. Res. Appl. www.ijera.com*, vol. 5, no. 10, pp. 93–98, 2015.
- [8] M. Ramezanizadeh, M. Alhuyi Nazari, M. H. Ahmadi, and K. wing Chau, "Experimental and numerical analysis of a nanofluidic thermosyphon heat exchanger," *Eng. Appl. Comput. Fluid Mech.*, vol. 13, no. 1, pp. 40–47, 2019.
- [9] M. Sandeep, A. Abinay, and P. J. Kumar, "Analysis and fabrication of heat pipe and thermosyphon," *Int. J. Mech. Eng. Technol.*, vol. 8, no. 12, pp. 160–172, 2017.
- [10] B. M. Jibhakate and M. Basavaraj, "Study of Parameters Affecting the Thermal Performance of Heat Pipe-A Review," *Int. J. Eng. Res. Technol.*, vol. 3, no. 19, pp. 9–11, 2015.
- [11] W. W. Wits and G. J. te Riele, "Modelling and performance of heat pipes with long evaporator sections," *Heat Mass Transf. und Stoffuebertragung*, vol. 53, no. 11, pp. 3341–3351, 2017.
- [12] S. H. Yoon and C. S. Lee, "Experimental investigation on the combustion and exhaust emission characteristics of biogas-biodiesel dual-fuel combustion in a CI engine," *Fuel Process. Technol.*, vol. 92, no. 5, pp. 992–1000, 2011.
- [13] J. Jose and R. Baby, "Recent advances in loop heat pipes: A review," *IOP Conf. Ser. Mater. Sci. Eng.*, vol. 396, no. 1, 2018.
- [14] M. A. Boda, T. B. Shaikh, and S. N. Sayyed, "Innovative Developments and Heat," vol. 3, no. 6, pp. 319–322, 2018.
- [15] P. Z. Shi, K. M. Chua, S. C. K. Wong, and Y. M. Tan, "Design and performance optimization of miniature heat pipes in LTCC," *J. Phys. Conf. Ser.*, vol. 34, no. 1, pp. 142–147, 2006.
- [16] A. . Chaudhari, M. D. Borkar, A. Deshpande, M. V. Tendolkar, and V. K. Singh, "Effect of Wick Microstructures on Heat Pipe Performance A Review," *SSRN Electron. J.*, pp. 1–8, 2018.



- [17] J. V. Suresh, P. Bhramara, and S. S. Krishna, "Effect of Working Fluid on Thermal Performance of Closed Loop Pulsating Heat Pipe," *Int. J. Eng. Adv. Technol.*, vol. 9, no. 2, pp. 953–956, 2019.
- [18] C. E. Andraka, T. A. Moss, V. Baturkin, V. Zaripov, and O. Nishchyk, "High-performance felt-metal-wick heat pipe for solar receivers," *AIP Conf. Proc.*, vol. 1734, 2016.